

An Implementation of Solar PV Array Based Multifunctional EV Charger

S Srikanta Deekshit¹, D Sai Krishna Kanth², P.Dastagiri³, A. Jayanth Naidu⁴, G.Shiva kumar⁵, C.Sai Praneeth Kumar Reddy⁶

1, 2 (Assistant Professor, Electrical and Electronics Department, Annamacharya Institute of Technology and Sciences, Rajampet

Email: deekshitkoushika@gmail.com)

3, 4, 5, 6 (UG Student, Electrical and Electronics Department, Annamacharya Institute of Technology and Sciences, Rajampet
Email: dastagiri017@gmail.com)

Abstract:

The charger is enabled to operate autonomously using a PV array for providing an uninterrupted charging and power to household loads. However, in the absence of the PV array or insufficient PV array generation, the grid connected mode of operation is presented. Moreover, the charger is supported with the synchronization and seamless mode switching control, so that the charger automatically connects/disconnects from the grid without disturbing the EV charging and household supply. The charger is also enabled with the vehicle-to-grid (V2G) active/reactive power support to the grid and vehicle-to-home (V2H) power transfer for supporting the local loads in an islanded condition.

Keywords — Electric vehicle, bi-directional charger, solar PV generation, reactive power, power quality.

I. INTRODUCTION

In the current scenario, the electric vehicle (EV) is emerging as a promising solution to the problems caused by fossil fuel powered vehicles. However, the adaptability of EV depends on the charging infrastructure. The charging of EV requires a huge amount of electrical energy, which mostly comes from coal/ gas-based power plants. Therefore, in a true sense, the EVs can be a green and clean alternative to the present transport system when the electrical energy required for the charging of EV, comes from the renewable energy sources such as solar, wind etc.. The advantage of this kind of charging station is that the PV array power is generated and used locally. Because of this, the transmission lines need not be upgraded for the high power. Moreover, the charging station does not require to draw power from the grid when the cost of energy is high. Another advantage of PV array-based charging station is that it is not location-specific. The use of office building and parking area for laying down the solar PV panels, as these solar PV panels also work as a shed and prevent the heating of the

vehicles and buildings. Therefore, the use of PV array-based charging station not only avoids overloading of the grid, but it also minimizes the operational cost of the charging station. Moreover, the coordinated operation of the PV array and EV mitigates the impacts of PV generation on the utility, and it eliminates the problems caused by the solar PV generation intermittency. Moreover, this topology is a kind of retrofit solution wherein the PV array can be augmented to the existing charging infrastructure with minimum change in the software (maximum power point tracking control algorithm) alone. However, if the charger is used only for charging the EV, the charger remains idle for at least 50% of the lifetime. Therefore, the converter of the charger has to be used for other tasks to improve the operational efficiency of the charger when the EV is not connected for charging. There are many functionalities proposed in the literature such as the four-quadrant operation of charger, vehicle-to-home operation using the EV battery and active filtering etc.. However, in the available literature, different converters and controls are used for different modes of operation. Moreover, the charger operation is restricted by the grid availability (islanded or grid connected operation), types of mode switching

among different operating modes (seamless or discontinuous) and these conditions affect the operational efficiency of the charger. Many efforts are being made to develop an integrated system with the capability to perform the above functionalities, which are beneficial to the grid, household loads and the EVs. In this paper, a household load integrated, grid connected solar PV array-based multifunctional EV charger is implemented with the combined control for achieving the satisfactory operation of various functionalities such as i) PV array MPPT without dc-dc converter, ii) four-quadrant operation of charger (V2G/G2V), iii) V2H with nonlinear load, iv) active filtering, v) islanded/grid connected operation, vi) synchronization (automatic mode switching), vii) MPPT derating, viii) PCC voltage correction etc. However, an integration of EV charging with a renewable source, household load and the grid, creates challenges for the energy management in the overall system. A dc-link voltage regulation based energy management scheme is proposed, which uses only present dc-link voltage information for effective energy management. Power factor correction in ac-dc converter using the adaptive intermediate bus voltage, in which proportional-integral (PI) control is used to regulate the dc-link voltage. The strategy for cancelling the second harmonic ripple in the dc-link voltage for designing the enhanced dc voltage control loop. However, the gains of the PI controller are fixed during the operation. Due to which, the tuning of the PI controller for accommodating the unknown disturbances, during the operation is not possible. Therefore, in this paper, a sliding mode control (SMC) is used for dc-link voltage regulation, so that both dynamic and steady-state performances of the system are improved. SMC is known for its excellent dynamic response and strong robustness to disturbances and uncertainties, such as unknown variations of control variables and system parameters. The main contribution of this work involves assimilating various functionalities such as i) PV array MPPT without dc-dc converter, ii) four-quadrant operation of charger (V2G/G2V), iii) V2H with nonlinear load, iv) active filtering, v) islanded/grid connected, vi) synchronization (automatic mode switching), vii) MPPT derating, viii) PCC voltage correction, in a single EV charger

configuration, without the need of additional dc-dc converter for PV array, thereby reducing the cost of charger and improving the reliability of the charging and household supply. The advantage of this system is that a single system meets the requirements of household load, EV and the utility.

II. THE MAIN FEATURES OF THIS SYSTEM ARE AS FOLLOWS.

- The use of PV array energy for EV charging and powering the household load, simultaneously in islanded and grid connected mode.
- Development of robust control strategy for generating a sinusoidal voltage at PCC, with total harmonic distortion (THD) less than 5%.
- The use of EV battery energy for supplying the household load uninterruptedly in islanded mode using vehicle-to-home (V2H) functionality.
- Design of control for synchronizing the grid and PCC voltage and logic for generating the switch enabling logic (E) for a seamless transition between islanded to grid connected mode.
- Active power filter operation using VSC, so that the charger does not pollute the grid.
- On-demand vehicle-to-grid (V2G) reactive power capability using the VSC and the EV battery.
- In grid connected mode, voltage and current always comply with the IEEE-519 standard.
- Capability to operate under distorted voltage condition.
- A dc link voltage regulation based energy management strategy for all operating modes.
- A sliding mode control based robust dc-link voltage regulation, so that the energy management scheme performs its aforementioned tasks.

III. SYSTEM CONFIGURATION

The circuit topology of the presented charging system is shown in Fig. 1. This system is a single-phase bi-directional charger for an EV that integrates the solar PV array directly on the dc-link of the VSC. This system charges the EV battery using the solar PV power/the grid power and feeds the solar PV / EV battery power into the grid. This charger is a two-stage charger, i.e. a bi-directional ac-dc conversion followed by the bi-directional dc-dc conversion stage. The ac-dc conversion stage converts the input

ac voltage into the dc voltage while charging the EV battery and works as an inverter to change the dc voltage into the ac voltage while feeding the solar PV power and EV power into the grid. The EV battery is connected to the output of the bi-directional dc-dc converter (BDDC). The dc-dc converter in this charger accomplishes the various tasks. While charging the EV battery, the dc converter works in buck mode and operates in boost mode while discharging the EV battery.

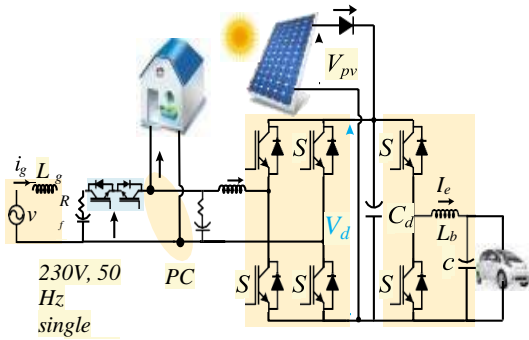


Fig. 1 Circuit topology of the charger

Moreover, it also regulates the dc bus voltage and harnesses the maximum generated power from the solar PV array. The charger is connected to the grid through the coupling inductor (L_c). It is needed to eliminate the harmonics and to smoothen the grid current. A ripple filter is also connected at the PCC (Point of Common Coupling) to prevent the injection of switching harmonics generated by the VSC into the grid.

IV. RESULTS AND DISCUSSION

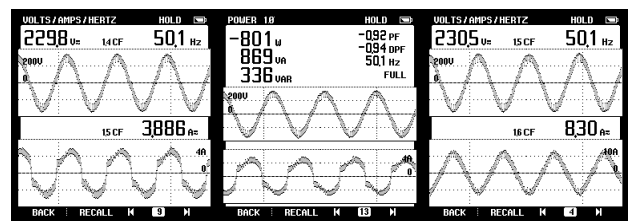
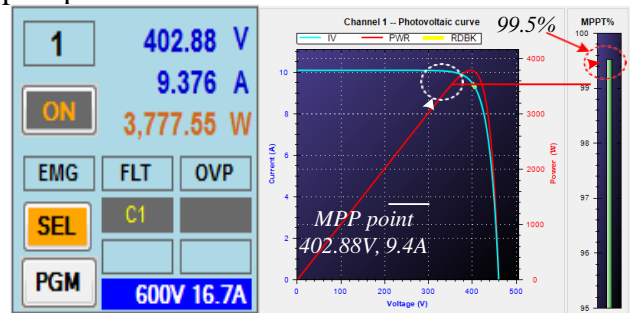
The EV charger designed for single-phase 230V, 50Hz grid is shown in Fig. 5. The open-circuit voltage and short circuit current of the solar PV array is 460V and 10A, respectively. However, the maximum power point voltage and current are 396 V and 9.5A, respectively. The lead-acid battery of 240V, 35Ah is used as an EV battery in the experimental prototype. The implementation of the charger is carried out using the digital controller (dSPACE-1006). For the implementation of the control algorithm, the digital controller requires various (voltage and current) signals of the charger. Therefore, various voltage and current signals (analog) are acquired using the Hall Effect based voltage (LEM LV-25P) and current (LEM LA- 55P)

sensor. These signals are converted into digital signals using an analog to digital converter (ADC). The digital controller uses the digital signal to implement the control algorithm and to generate the switching pulses for VSC and dc-dc converter.

The performance of the charger is shown in Figs. 6-13. The performance of the charger is evaluated in both steady-state and dynamic conditions. The steady-state performance of the charger is presented for the case when the solar PV array energy is used to charge the EV, feeds the local household load and supports the grid with surplus power. The dynamic performance of the charger is presented for various operating modes in both islanded and grid connected conditions. During implementation, the solar PV array power (PPV), the power drawn from the grid (Pg), and the power drawn from the EV (PEV), are considered positive. However, the power fed into the grid, power drawn by the load and power drawn for EV charging is considered negative.

A. Steady-State Performance of Charger

Fig. 6 shows the experimental results in a steady-state condition. The steady-state behavior of the charger is presented for the GCM, when the solar PV array power (Ppv) is used for EV charging, powering the local load and supporting the grid with the surplus power.



(c) (d) (e)

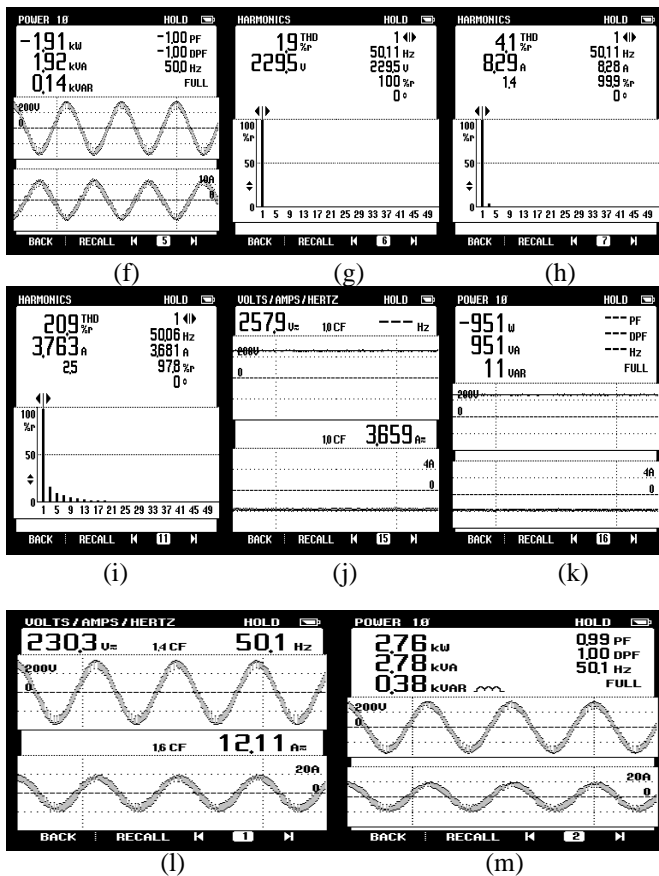


Fig. 6 Steady state performance in grid connected mode, (a)-(b) VPV, IPV and PPV, (c)-(d) v_h , i_h and P_h , (e)-(f) v_g , i_g and P_g , (g)-(i) harmonic spectrum of v_g , i_g and i_h , (j)-(k) V_{ev} , I_{ev} and P_{ev} , (l)-(m) v_c , i_c and P_c .

Figs. 6 (a)-(b) show that the solar PV array is generating 3.77kW. Out of 3.77 kW, 0.8kW is taken by the household load (P_h) and 0.95kW is used by the EV for charging. Remaining 1.91kW is fed into the grid at UPF. The voltage (VPV), current (IPV) and power (PPV) of the solar PV array are shown in Figs. 6(a)-(b). The voltages, currents and powers of the load and the EV battery are shown in Figs. 6 (c)-(d) and Figs. 6 (j)-(k). The voltage (v_g), current (i_g), and power of the grid (P_g) are shown in Figs. 6 (e)-(f). The charger is not injecting any voltage and current harmonics into the grid as shown by the grid voltage (v_g), grid current (i_g) and load current (i_h), total harmonic distortion (THD) in Figs. 6 (g)-(i). Moreover, it is also not drawing any reactive power from the grid as justified by the unity displacement power factor (DPF) operation of the charger in Fig. 6 (f). Fig. 6 (l)-(m) show the VSC parameters.

B. Dynamic Performance of Charger

The islanded mode of the charger is presented to show the charger capability to operate autonomously using the solar PV array energy for providing the charging facility to the EV and supply to the household load. During the islanded mode of operation, the household load changes along with the solar irradiance. Therefore, the charger performance under these disturbances is presented in Fig. 7. Initially, the solar PV array charges the EV and feed the household load as shown by the negative EV current in Fig. 7(a). However, after some time, the solar PV array generation (P_{pv}) becomes zero. Therefore, to feed the load uninterruptedly, the EV battery starts discharging, to support the home loads, as shown by the positive battery current (I_{ev}) in Fig. 7 (a). This mode is called vehicle to home. Fig. 7 (b) shows the voltage generated at the PCC (v_s) using the charger. Moreover, the non-sinusoidal load current (i_h) is also exhibited in Fig. 7 (b). Fig. 7(b) exhibits that during solar irradiance change the PCC voltage (v_s), load current (i_h) and dc-link voltage (V_{dc}) are undisturbed.

The islanded operation under load change is shown in Figs. 7(c)-(d). Here, the load is changed in step over a wide range. The dc-link voltage is maintained by the bi-directional dc-dc converter, the load change is compensated by the EV battery. Because of which, the EV battery charging changes with the load change. However, the solar PV array generation (P_{pv}) and the dc-link voltage (V_{dc}) are not affected by the load change. Fig. 7(d) also shows that the connection/disconnection of the household load is not disturbing the PCC voltage. Fig. 7 (d) shows that when the load is disconnected, the whole solar PV array power (P_{pv}) is stored into the EV battery. However, the MPP operation of the solar PV array is not affected.

In Figs. 7 (e)-(f), the solar irradiance is changed in steps, keeping the household constant. Initially, with the increase in solar irradiance, PV power increases. As a result, the power stored in the EV battery also increases to maintain the active power balance. However, when the solar irradiance is increased from 500W/m² to 1000W/m², the solar PV array generation does not increase because the controller increases the reference dc-link voltage to achieve the

MPPT derating as the charging rate of EV is restricted by the controller as shown in Fig. 7.

The charger operates in grid connected mode either due to the excess power generation or power scarcity. In both cases, the charger exchanges the power with the grid at unity power factor. However, in grid connected mode also, many disturbances occur during the operation. Therefore, the stable operation of the charger under this operating condition is required. The behavior under the load perturbation in GCM is shown in Fig.

8. In grid connected mode, the dc-link voltage is regulated by the voltage source converter of the charger, therefore, the load change only affects the grid power. Here, the load is changed in steps and the corresponding change in grid power (P_g) can be seen in Fig. 8(a). The reduction in load current (i_h) is causing an increase in grid current (i_g) as shown in Fig. 8(b). However, the PV array current (I_{pv}) and the EV charging current (I_{ev}) are not affected by the load change. The same is justified by the undisturbed PV array (P_{pv}) and the EV power (P_{ev}). The voltage across the dc link (V_{dc}) is also regulated during the load change. The performance under solar irradiance change is shown in Figs. 8(c)-(d). Due to the change in the solar irradiance level, the PV array generation (P_{pv}) changes. Since the household loads and the EV charging should not be disturbed by the irradiance change, the grid power (P_g) changes to maintain the power balance. The solar irradiance is changed in step from 1000W/m² to 700W/m², 700W/m² to 300W/m² and so on. Due to this, the grid power (P_g) becomes both positive and negative. That means, at 1000W/m², the excess generation is supplied back to the grid. However, at 300W/m², the power is drawn from the grid. The EV power (P_{ev}), load power (P_h) and dc-link voltage (V_{dc}) remain undisturbed.

In GCM, the EV charger participates in demand based active power exchange with the grid. Therefore, the EV voluntarily takes active power from the grid or discharges some of its stored energy to the grid as shown in Figs. 8 (e)-(f). Due to the charging /discharging of the EV battery, the grid power (P_g) changes without affecting the PV array generation (P_{pv}) and the load supply (P_h). Figs. 8(e)-(f) show the step change in the battery current (I_{ev}) from charging to discharging. Due to the discharging of the battery, the grid current (i_g) increases.

However, the PV array current (I_{pv}) and the dc-link voltage (V_{dc}) remain unaltered. Therefore, from the dynamic results, it is observed that the charger operation in grid connected and islanded mode are not affected by the disturbances. Moreover, it is also perceived that one type of perturbation is not interfering with the operation of another component.

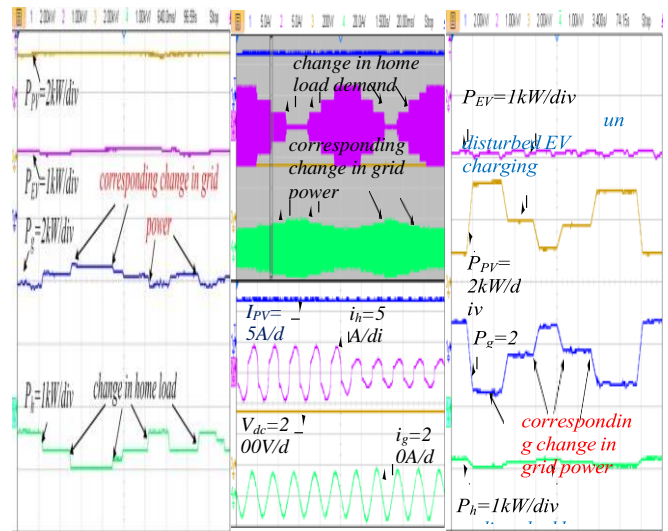


Fig. 9 shows the V2G reactive power performance at $P_g=0$ kW. Due to the step-change in the reference reactive power (Q_{ref}) from 1kVAR to -1kVAR, the grid current (i_g) becomes leading from lagging. Moreover, the dc-link voltage (V_{dc}) remains undisturbed.

Fig. 10 shows the harmonic compensation and PCC voltage correction capability of the charger. Fig. 10 shows that the grid current (i_g) is the same as load current (i_h) without harmonics mitigation using VSC. However, it is observed that the grid current (i_g) becomes sinusoidal after harmonics compensation. The current (i_s) of VSC is shown in Fig. 10. Moreover, it is observed that the PCC voltage (v_g) profile also improves due to compensation.

Fig. 11 shows the performance of mode switching control and enabling signal (E) generation after synchronization. From Fig. 11, it is observed that the charger is automatically switching the mode between islanded and grid connected modes without affecting the power to the household load. Moreover, during the connection to/disconnecting from the grid, the grid current (i_g) is smooth.

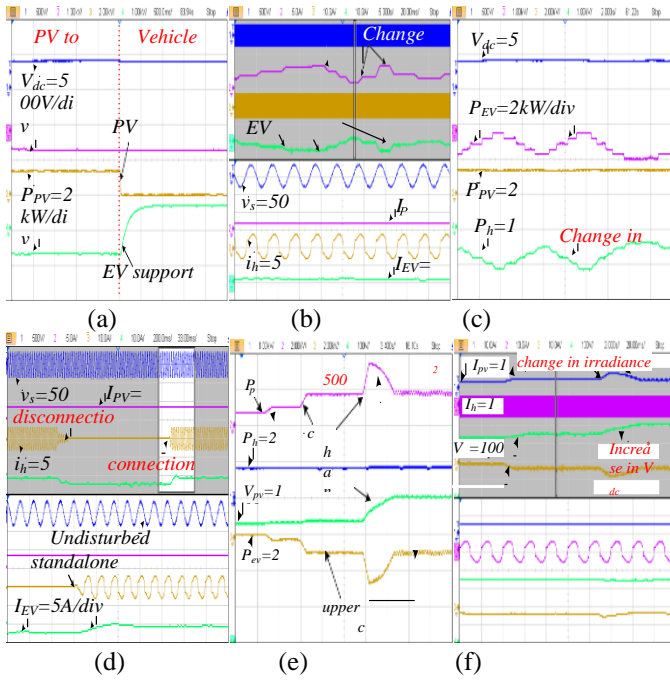


Fig. 7 Dynamic performance in islanded condition, (a)-(b) under solar irradiance change, (c)-(d) under the change in household load, (e)-(f) derating of MPPT

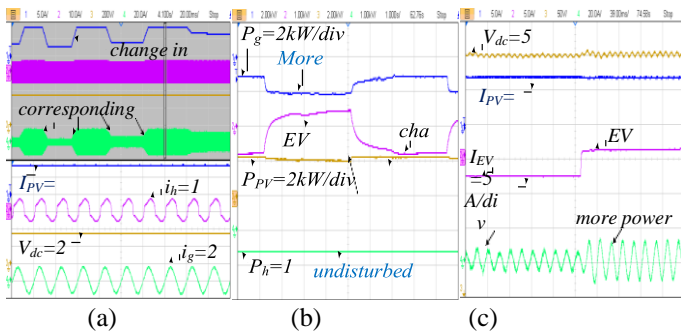


Fig. 8 Dynamic performance in grid connected mode, (a)-(b) under change in household load, (c)-(d) under change in solar irradiance power, (e)-(f) under change in charging/discharging of EV battery

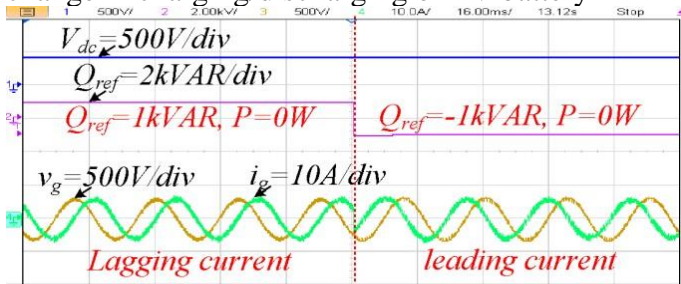


Fig. 9 Performance of vehicle to grid reactive power support

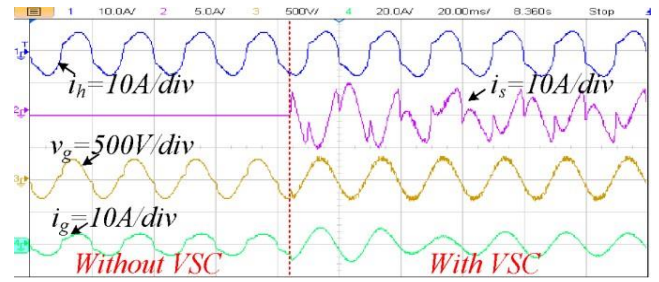


Fig. 10 Performance under distorted voltage condition and active power filter operation

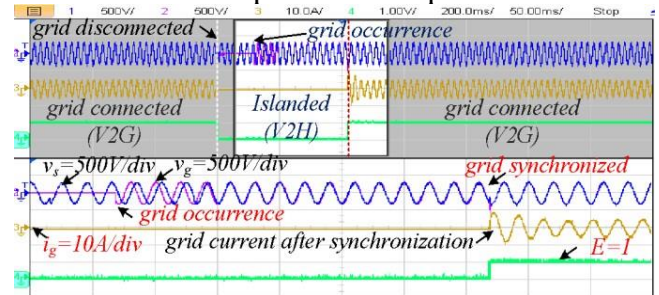


Fig. 11 Synchronization, mode switching and enabling signal generation

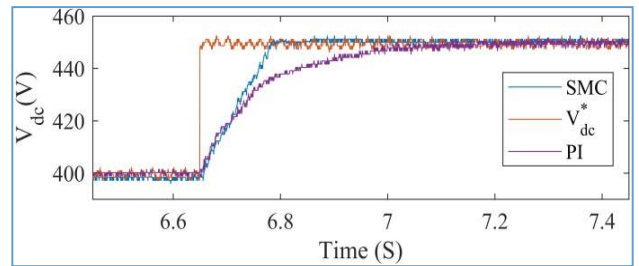
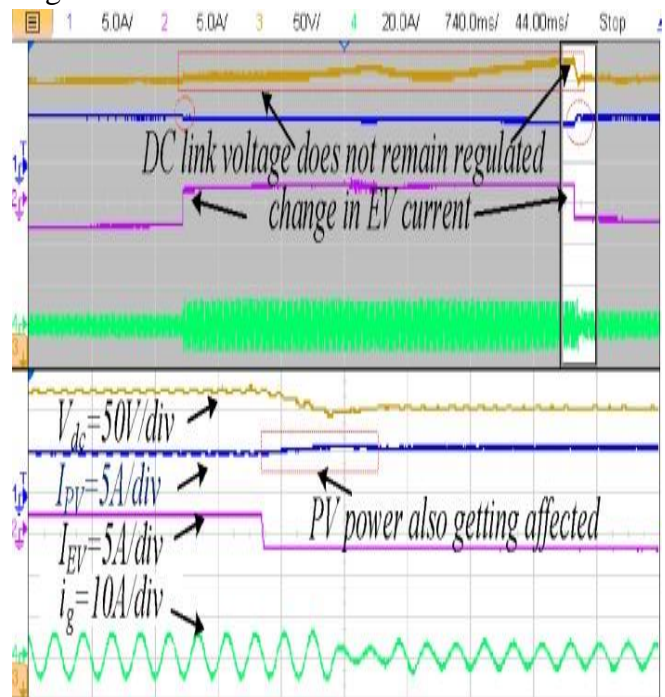


Fig. 12 Comparison of dc-link voltage regulation using PI and SMC control



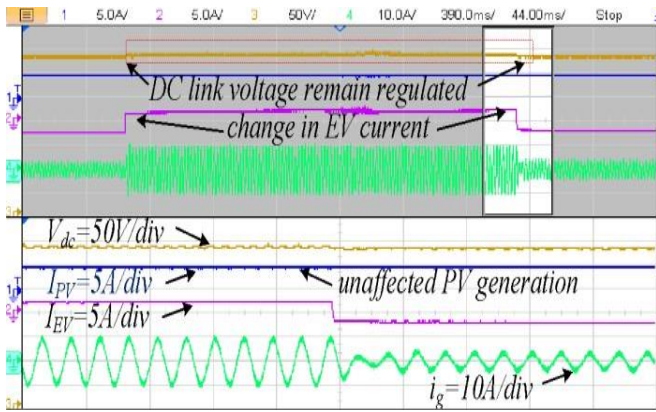


Fig. 13 Performance comparison under the sudden change in charging/discharging current of EV, (a) PI control, (b) SMC control

C. Comparison of dc Link Voltage Regulation Using PI Control and SMC Control

Fig. 12 shows the dc-link voltage (V_{dc}) regulation capability of the PI controller and SMC under the step change of 50V in reference dc-link voltage (V^*). From Fig. 12, it is observed that the SMC is faster in regulating the dc-link voltage as compared the PI control.

D. Performance Comparison of SMC and PI Control at Sudden Change in Charging/Discharging Current of EV

Due to sudden variation in EV current (I_{ev}) from discharging to charging, the dc-link voltage (V_{dc}) is not regulated with the PI control, as shown in Fig. 13 (a). However, the SMC control has regulated the dc-link voltage (V_{dc}) at the sudden change, as shown in Fig. 13 (b). Since the PV array MPP operation depends on the dc-link voltage regulation at MPP voltage; the PV array does not operate at MPP due to the steady-state error in PI control. Moreover, it also changes under the sudden change in EV current. However, with SMC, the steady-state error is always zero and it also does not change with EV current change. Therefore, it always operates at MPP.

V. CONCLUSIONS

An integrated charger with solar PV array, household load and grid has been implemented using the IGBT switches-based converters, solar simulator, EV battery, dSPACE (1006) controller and the test results have verified the simultaneous EV charging and household supply in both islanded and grid connected modes. From these test results, it is

observed that this charger is performing its specified task of EV charging, supplying local loads and maintaining the power quality at the grid side. Moreover, the islanded operation with voltage THD less than 5% and vehicle to home operation using solar PV array is also verified. The demand-based reactive power support and the active power filtering using VSC are also validated through test results. The smooth transition from islanded to grid connected mode and vice versa are verified by test results.

REFERENCES

1. J. R. Aguero, E. Takayesu, D. Novosel and R. Masiello, "Modernizing the Grid: Challenges and Opportunities for a Sustainable Future," *IEEE Power and Energy Magazine*, vol. 15, no. 3, pp. 74-83, May-June 2017.
2. D. Bowermaster, M. Alexander and M. Duvall, "The Need for Charging: Evaluating utility infrastructures for electric vehicles while providing customer support," *IEEE Electrifi. Mag.*, vol. 5, no. 1, pp. 59-67, 2017.
3. X. Lu and J. Wang, "A Game Changer: Electrifying Remote Communities by Using Isolated Microgrids," *IEEE Electrifi. Mag.*, vol. 5, no. 2, pp. 56- 63, June 2017.
4. T. Ma and O. A. Mohammed, "Optimal Charging of Plug-in Electric Vehicles for a Car-Park Infrastructure," *IEEE Trans. Ind. Applicat.*, vol. 50, no. 4, pp. 2323-2330, July-Aug. 2014.
5. L. Cheng, Y. Chang and R. Huang, "Mitigating Voltage Problem in Distribution System With Distributed Solar Generation Using Electric Vehicles," *IEEE Trans. Sust. Ene*, vol. 6, no. 4, pp. 1475-1484, Oct. 2015.
6. S. J. Gunter, K. K. Afridi and D. J. Perreault, "Optimal Design of Grid- Connected PEV Charging Systems With Integrated Distributed Resources," *IEEE Trans. Smart Grid*, vol. 4, no. 2, pp. 956-967, 2013.
7. A. S. Satpathy, N. K. Kishore, D. Kastha and N. C. Sahoo, "Control Scheme for a Stand-Alone Wind Energy Conversion System," *IEEE Trans. Energy Conversion*, vol. 29, no. 2, pp. 418-425, June 2014. Nov. 2018.
8. O. Erdinc, N. G. Paterakis, T. D. P. Mendes, A. G. Bakirtzis and J. P. S. Catalão, "Smart Household Operation Considering Bi-Directional EV and ESS Utilization by Real-Time Pricing-Based DR," *IEEE Trans. Smart Grid*, vol. 6, no. 3, pp. 1281-1291, May 2015.
9. H. R. Baghaee, M. Mirsalim, G. B. Gharehpetian and H. A. Talebi, "A Decentralized Power Management and Sliding Mode Control Strategy for Hybrid AC/DC Microgrids including Renewable Energy Resources," *IEEE Trans. Ind. Informatics*. Early Access.
10. Z. Yi, W. Dong and A. H. Etemadi, "A Unified Control and Power Management Scheme for PV-Battery-Based Hybrid Microgrids for Both Grid-Connected and Islanded Modes," *IEEE Trans. Smart Grid*, vol. 9, no. 6, pp. 5975-5985, Nov. 2018.